Interface hybridization and spectral distribution in strongly correlated itinerant magnetic systems

Changfeng Chen
Department of Physics, University of Nevada, Las Vegas, Nevada 89154
(Received 6 May 1994; revised manuscript received 1 July 1994)

We report the results of a theoretical study of the effect of the interface *s-d* hybridization on the photoemission spectral distribution in a one-monolayer Co on Cu(001) structure. The single-particle electronic structure and many-body interactions are treated on an equal footing in a numerical scheme that incorporates both band-structure and interaction effects. Using exact diagonalization method on small clusters with periodic boundary conditions, spin- and angle-resolved photoemission spectra are calculated. We study the effect of the interface hybridization on the spectral distribution by first calculating the spectra of an unsupported Co(001) monolayer in the absence of the substrate. Then we calculate the spectra with the substrate included. In the latter case, the *s-d* hybridization is first turned off to isolate the contribution from the crystal-field effect. Eventually, the one-monolayer Co on Cu(001) with full interface *s-d* hybridization, the realistic system, is studied. The calculated spectra are analyzed in a many-body picture and compared to available experimental data. Further experimental measurements are called for to test some theoretically predicted features.

I. INTRODUCTION

Modern ultrahigh vacuum technology has made it possible to grow ultrathin magnetic overlayers on various substrates in a well-controlled manner. A lot of recent effort has focused on 3*d* magnetic transition metal overlayers.[1] Besides their obvious importance in current technological applications, it is expected that these atomic-scale engineered systems may exhibit novel properties of interest to both fundamental studies of physics and potential new applications. These systems are often probed by various spectroscopic measurements to determine the underlying electronic and magnetic structures. While theoretical understanding of the spectroscopy for ideal noninteracting and practical weakly interacting systems is well established, it takes careful modeling, computation, and interpretation to understand the spectra of strongly correlated systems like 3*d* magnetic transition metal systems and extract correct physics. A well-known early example is the discovery[2] of the "satellite" peak in the photoemission spectrum (PES) of Ni and the subsequent theoretical explanation[3] of its many-body origin. In most of the original theoretical work various perturbative approaches that involve *ad hoc* approximations on the interaction terms in the Hamiltonian were used. Nevertheless, they successfully explained the experimental observation and, more importantly, established the understanding that the *d-d* interaction is responsible for driving spectral weight to binding energies beyond the range predicted by single-particle theories. More recently, various numerical schemes have been developed to study many-body effects in spectroscopic processes in strongly correlated systems. To this end, a lot of recent work has focused on some ideal models, such as the single-band Hubbard model[4] with Hamiltonian parameters chosen arbitrarily or determined by band calculations.[5] In connection with the high-temperature superconducting cuprates, some more realistic, multiband models also have been studied.[6]

Recently we have developed a systematic theoretical-computational approach to include realistic band aspects into a tight-binding-type model.[7] Single-particle parameters are obtained by fitting to the results of all-electron band-structure calculations; interaction parameters allowed by atomic symmetry are included and determined by atomic data and the constraints imposed by metallic screening in the solids. This approach treats single-particle and many-body effects on an equal footing and provides results complementary to both band calculations and many-body calculations on simple model systems. It allows one to study many-body correlation effects in specific real materials of interest and distinguishes many-body effects from those caused by single-particle terms. This approach has been successfully applied to various thin-film and surface systems of 3*d* transition metals.[7,8] Most recently we have generalized this approach to the study of the overlayer-substrate interaction. Here the focus is on the effect of the interface hybridization between the 3*d* electrons in the transition metal overlayer and *s* electrons in the substrate. In a recent Rapid Communication[9] we have presented a brief account of the calculated photoemission spectrum of one-monolayer Co on Cu(001). It has revealed some very interesting many-body effects driven by the *d-d* interaction in the Co layer but modified by the interface Co *d*–Cu *s* hybridization. In this paper we report in more detail the construction of the model, the theoretical and computational treatment of the single-particle and many-body terms in the Hamiltonian, and the calculated photoemission spectra. In addition to the previously reported normal-emission photoemission results we also have calculated the spectrum corresponding to the $\bar{X}$ point in the surface Brillouin zone to study the angular dependence

0163-1829/94/50(19)/14539(7)/$06.00

of the effect of the interface hybridization on the spectrum. Furthermore, to clearly identify the effect of the interface hybridization, we have calculated the PES for the following three different configurations of the Co/Cu system. First, a single *unsupported* Co layer is studied. The purpose is to establish the features in the PES in the pure two-dimensional system in the absence of the Cu substrate. Then it is put on top of the Cu substrate but without the *s-d* hybridization. The change in the spectrum due to crystal-field effects is studied. Finally the *s-d* hybridization is turned on and the PES of the realistic one-monolayer Co on Cu(001) is calculated. The calculated results are analyzed in terms of both single-particle and many-body correlation effects and the PES of the realistic one-monolayer Co on Cu(001) is compared to available normal-emission experimental data.

In the next section we introduce the Hamiltonian and the method of calculation. In Sec. III, we present the results and discussion. Finally we give conclusions in Sec. IV.

II. HAMILTONIAN AND METHOD OF CALCULATION

The theoretical method used in this work is the small-cluster approach.[10] A cluster of a finite (usually small) number of atoms with periodic boundary conditions is used to model an infinite system. It is equivalent to sampling a few high-symmetry points in the Brillouin zone. This method has been widely used in the study of strongly correlated systems. Its advantage is that there is no approximation applied to the Hamiltonian. Quantum many-body problems are solved *exactly* in the numerical form. Therefore it provides accurate information about the many-body effect in the system. Its limitation is also obvious. Due to exponential growth of many-body states with the system size, only very small systems can be studied using this approach. In practice, since many spectroscopic processes are fast and intrinsically short ranged they can be well described by the small-cluster approach. Numerous works on this subject have been reported. It is now generally accepted that the sudden (one-step) approximation and small-cluster approach provide rather accurate description of many interacting systems, although careful modeling and insightful interpretation of the calculated results are always required.

In this work, we choose a tetrahedral cluster, the smallest nontrivial fcc crystal, and apply periodic boundary conditions in two dimensions to construct the fcc Co/Cu(001) structure. In this structure, the two Co sites are in the top layer and the two Cu sites in the bottom layer. Only the interface Cu layer is *explicitly* included to allow the electron (hole) hopping between the Co and Cu sites. The bulk layers of Cu provide a crystal field that is considered in the calculation. In the case of a sinlge layer of fcc Co, the Cu layer is simply removed. We only *explicitly* include the Co *d* and Cu *s* orbitals and the nearest-neighbor interactions in the calculation. The interactions between the Co *s*, *p*, and *d* electrons and beyond the nearest neighbors are effectively considered by adjusting the *d*-orbital energies to produce the ground-state properties, e.g., magnetization. The Cu *d* band is centered well below the Fermi level and has negligible influence on the results. Since it is estimated[11,18] that one monolayer of Co on Cu(001) has a magnetic moment of about $1.8\mu_B$ (μ_B is the Bohr magneton) per Co atom and the small-cluster approach allows only an integral number of particles in the cluster, we consider in the neutral state two *d* holes per Co atom.

The Hamiltonian consists of both single-particle and two-particle terms. It is written as

$$H = \sum_{i,j;\mu,\nu;\sigma} t_{i\mu,j\nu} c^{\dagger}_{i\mu\sigma} c_{j\nu\sigma} + \sum_{i;\mu;\sigma} E_{\mu} c^{\dagger}_{i\mu\sigma} c_{i\mu\sigma} + \sum_{i;\mu,\nu,\lambda,\phi;\sigma,\sigma'} V_{\mu\nu\lambda\phi} c^{\dagger}_{i\mu\sigma} c^{\dagger}_{i\nu\sigma'} c_{i\lambda\sigma'} c_{i\phi\sigma}, \quad (2.1)$$

where $c^{\dagger}_{i\mu\sigma}$ ($c_{i\mu\sigma}$) are *hole* creation (annihilation) operators. The indices i, j label atoms in the cluster; μ, ν, λ, and ϕ label the Co *d* and Cu *s* orbitals; σ, σ' are spin labels. The first two terms are single-particle hopping and orbital-energy terms, and the third terms describes the intra-atomic interaction *on the Co sites only*. The single-particle parameters for Co and Cu are obtained according to the Slater-Koster scheme.[12] They are adjusted to reproduce, in the absence of interactions, the calculated *paramagnetic* local-density-approximation (LDA) band structure[13] at selected high-symmetry points in the surface Brillouin zone. For the matrix elements between Co and Cu, we take the geometric mean of the respective Co-Co and Cu-Cu matrix elements. The intra-atomic interactions, which is the dominant contribution,[14] include three terms: a direct Colomb integral U for two particles on the same *d* orbital, an exchange integral $J_{t_{2g}}$ for two particles on two different t_{2g} orbitals, and another one J_{e_g} for two particles on two different e_g orbitals. The Coulomb interaction for two particles in different orbitals is $U' = U - 2J$. This formula applies to particles in all *d* orbitals. All intra-atomic *d-d* interactions are expressed in terms of U, an average exchange integral $J = (J_{t_{2g}} + J_{e_g})/2$, and an exchange anisotropy $\delta J = J_{e_g} - J_{t_{2g}}$. The bulk value of $U = 6.6$ eV (Ref. 15) is used in the calculation. Other interaction parameters are set in the ratios $U : J : \delta J = 40{:}8{:}1$, based on the consideration of the constraints imposed by the atomic data and the screening effect in metals. They are also chosen to produce correct ground-state magnetization. The calculated results are insensitive to exact values of these ratios.

There are five *d* orbitals per Co atom per spin; in the presence of a cubic field, as in a bulk fcc crystal, these orbitals split into a triplet t_{2g} and a doublet e_g. It is clear that the crystal-field effects are, in the unsupported monolayer structure and the overlayer structure, quite different from that of the bulk, because the atoms in these structures have fewer and different neighboring connections. A straightforward calculation is carried out to determine the shifts of the energy levels of the five *d* orbitals relative to the "center of gravity" of the *d* levels defined as $E^{\mathrm{Co}}_{\mathrm{CG}} = (3/5)E_{t_{2g}} + (2/5)E_{e_g}$, where $E_{t_{2g}}$ and E_{e_g} are the corresponding *d* level energies in bulk

Co. The shifts caused by the crystal-field effect in the unsupported monolayer structure are obtained as

$$\Delta E_\alpha = (4/15)d_{1n}^{\mathrm{Co}} + (4/15)d_{2n}^{\mathrm{Co}}, \tag{2.2}$$

$$\Delta E_\beta = -(16/15)d_{1n}^{\mathrm{Co}} + (44/15)d_{2n}^{\mathrm{Co}}, \tag{2.3}$$

$$\Delta E_\gamma = (44/15)d_{1n}^{\mathrm{Co}} - (16/15)d_{2n}^{\mathrm{Co}}, \tag{2.4}$$

$$\Delta E_\delta = \Delta E_\epsilon = -(16/15)d_{1n}^{\mathrm{Co}} - (16/15)d_{2n}^{\mathrm{Co}}, \tag{2.5}$$

where the subscripts α, β, γ, δ, and ϵ refer to the five d orbitals of symmetry $r^2 - 3z^2$, $x^2 - y^2$, xy, yz, and zx, respectively. The parameters d_{1n}^{Co} and d_{2n}^{Co} are the contributions to the energy shifts from each of the first and second neighbors in the structure. They are determined by applying this crystal-field effect analysis to the bulk Co structure and fitting to the band calculation results.[13] The same analysis yields wthe following results for the one monolayer of Co on Cu(001), which consist of the contributions from the Co atoms in the overlayer and those from the Cu atoms in the substrate:

$$\Delta E_\alpha = (4/15)d_{1n}^{\mathrm{Co}} - (11/15)d_{1n}^{\mathrm{ave}} + (4/15)d_{2n}^{\mathrm{Co}} + (16/15)d_{2n}^{\mathrm{ave}}, \tag{2.6}$$

$$\Delta E_\beta = -(16/15)d_{1n}^{\mathrm{Co}} - (1/15)d_{1n}^{\mathrm{ave}} + (44/15)d_{2n}^{\mathrm{Co}} - (4/15)d_{2n}^{\mathrm{ave}}, \tag{2.7}$$

$$\Delta E_\gamma = (44/15)d_{1n}^{\mathrm{Co}} - (16/15)d_{1n}^{\mathrm{ave}} - (16/15)d_{2n}^{\mathrm{Co}} - (4/15)d_{2n}^{\mathrm{ave}}, \tag{2.8}$$

$$\Delta E_\delta = \Delta E_\epsilon = -(16/15)d_{1n}^{\mathrm{Co}} + (14/15)d_{1n}^{\mathrm{ave}} - (16/15)d_{2n}^{\mathrm{Co}} - (4/15)d_{2n}^{\mathrm{ave}}, \tag{2.9}$$

where

$$d_{kn}^{\mathrm{ave}} = \sqrt{d_{kn}^{\mathrm{Co}} d_{kn}^{\mathrm{Cu}}}, \qquad k = 1, 2, \tag{2.10}$$

where d_{kn}^{Cu} (k = 1,2) are obtained by fitting to all-electron band calculation results for bulk Cu. As a result, the crystal-field contribution from *all* substrate Cu layers is included. All the Hamiltonian parameters are listed in Table I. The energies are measured *below* the Fermi level of bulk fcc Co for holes.

With five d orbitals per Co atom per spin and one s orbital per Cu atom per spin, there are 20 orbitals in the two-atom (Co) cluster for the unsupported Co(001) monolayer structure and 24 orbitals in the four-atom cluster for the one-monolayer Co/Cu(001) structure. Simple combinatorial arguments yield 4845 and 10 626 many-body states in the neutral state of the two clusters. The photoemission process introduces another hole, yielding 15 540 and 42 504 final states, respectively. The space and spin symmetries inherent in the Hamiltonian must be exploited in order to diagonalize the complete many-body Hamiltonian matrices. First, total spin and its z-component in the cluster are good quantum numbers. Spin operators are applied to sort out states with definite spin indices. Furthermore, space-group decomposition reduces the sizes of Hamiltonian matrices in a very efficient way.

TABLE I. The Hamiltonian parameters (measured in eV below the Fermi level of bulk fcc Co) for the one monolayer of Co on Cu(001) studied in this work. The numbers in parentheses are the d-orbital energies for the unsupported Co(001) monolayer. The s-d hybridization parameters are the geometric mean of the corresponding Cu and Co results.

$(dd\sigma)$	0.524
$(dd\pi)$	−0.433
$(dd\delta)$	0.138
E_α	1.550 (1.319)
E_β	1.818 (1.770)
E_γ	0.510 (0.037)
E_δ	1.774 (2.150)
E_ϵ	1.774 (2.150)
$(sd\sigma)_1$	0.471
$(sd\sigma)_2$	0.134
$(ss\sigma)_1$	1.022
$(ss\sigma)_2$	0.013
E_s	−1.097

The two clusters studied in this work have C_4 point-group symmetry at the surface. The space group is the direct product of the C_4 group and the finite translational group of the periodic-cluster structure which, in the present case, is a two-element group, consisting of the identical translation and the translation that connects the two atoms in the cluster in the same layer. This corresponds to sampling the $\bar{\Gamma}$ point, the center of the two-dimensional surface Brillouin zone, and the $\bar{X}$ point, the center of the zone boundary. Since there is no translational symmetry perpendicular to the layer [i.e., along the (001) direction], both clusters have the same space-group symmetry. The space group is of order 8. There are eight irreducible representations, four at the $\bar{\Gamma}$ and four at the $\bar{X}$ point. All representations are nondegenerate. However, two pairs, $\bar{\Gamma}_3$-$\bar{\Gamma}_4$ and $\bar{X}_3$-$\bar{X}_4$, are degenerate due to time-reversal symmetry. Table II lists the

TABLE II. The character table of the space group for the two clusters with periodic boundary conditions studied in this work. The point group of the cluster structures is of C_4 symmetry. There are two elements in the translational group: the identical translation and the translation τ that connects the two atoms in the clusters in the same layer.

	E	C_4	C_2	C_4^{-1}	$E;\tau$	$C_4;\tau$	$C_2;\tau$	$C_4^{-1};\tau$
$\bar{\Gamma}_1$	1	1	1	1	1	1	1	1
$\bar{\Gamma}_2$	1	−1	1	−1	1	−1	1	−1
$\bar{\Gamma}_3$	1	i	−1	$-i$	1	i	−1	$-i$
$\bar{\Gamma}_4$	1	$-i$	−1	i	1	$-i$	−1	i
$\bar{X}_1$	1	1	1	1	−1	−1	−1	−1
$\bar{X}_2$	1	−1	1	−1	−1	1	−1	1
$\bar{X}_3$	1	i	−1	$-i$	−1	$-i$	1	i
$\bar{X}_4$	1	$-i$	−1	i	−1	i	1	$-i$

TABLE III. Sizes of the Hamiltonian matrix blocks of the various particle number, spin, and space-group symmetries for the unsupported fcc Co(001) monolayer.

		$\bar{\Gamma}_1$	$\bar{\Gamma}_2$	$\bar{\Gamma}_3$	$\bar{\Gamma}_4$	$\bar{X}_1$	$\bar{X}_2$	$\bar{X}_3$	$\bar{X}_4$
$N=4$	$S=2$	28	30	26	26	24	24	26	26
	$S=1$	120	118	126	126	124	124	126	126
	$S=0$	113	112	100	100	100	100	100	100
$N=5$	$S=5/2$	34	32	30	30	34	32	30	30
	$S=3/2$	230	230	232	232	230	230	232	232
	$S=1/2$	414	416	410	410	414	416	410	410

character table of the space group. With a complete set of matrices that transform according to the irreducible representations, it is possible to project out sets of symmetrized basis states,

$$\Psi^j_{\mu S} = \sum_R \chi^\mu_R P_R \psi^j_S, \tag{2.11}$$

where ψ^j_S is the jth state in the subspace of spin S (S may describe *both* total and z component of spin), P_R the projection operator corresponding to the space-group element R, χ^μ_R the corresponding character, and $\Psi^j_{\mu S}$ the symmetrized basis state with definite spin S and spatial symmetry μ. Once the index j runs through the whole subspace, all the symmetrized states are sorted and properly normalized. Since group theory guarantees[16] that Hamiltonian matrix elements between states belonging to different irreducible representations are always zero, the original Hamiltonian matrix is now decomposed into smaller Jordan blocks. The resulting block sizes are shown in Table III and IV for the two structures studied in this work. It can be seen that the reduction of the matrix size is quite effective, which in turn drsatically reduces the computation time. The solutions obtained by diagonalizing these blocks are exact solutions of the full Hamiltonian for the clusters. In the computer codes for the projection of symmetrized states, we used a real-number-only algorithm. Since there are imaginary numbers involved in the character table, linear combinations of the projection operators of the degenerate irreducible representations (i.e., $\bar{\Gamma}_3$-$\bar{\Gamma}_4$ and $\bar{X}_3$-$\bar{X}_4$ pairs) are taken so that all characters used in the codes are real integers. The price for doing so is the doubling of the size of the matrix blocks. For examble, the largest block size for the one-monolayer Co-on-Cu(001) structure is actually (2134 × 2134) instead of (1081 × 1081) as listed in Table IV. However, since the ground state of the system ($N=4$) is fully spin polarized with $S=2$, the final state ($N=5$) can only have spin $S=5/2$ or $S=3/2$. Therefore, the largest Hamiltonian matrix we have to deal with numerically is of order 1306, corresponding to final states with $N=5$, $S=3/2$, and spatial symmetries $\bar{\Gamma}_3$-$\bar{\Gamma}_4$ and $\bar{X}_3$-$\bar{X}_4$. When dealing with larger matrices the codes can be modified to release this real-number-only restriction.

TABLE IV. Sizes of the Hamiltonian matrix blocks of the various particle number, spin, and space-group symmetries for the one monolayer Co-on-Cu(001) structure.

		$\bar{\Gamma}_1$	$\bar{\Gamma}_2$	$\bar{\Gamma}_3$	$\bar{\Gamma}_4$	$\bar{X}_1$	$\bar{X}_2$	$\bar{X}_3$	$\bar{X}_4$
$N=4$	$S=2$	62	65	64	64	56	56	64	64
	$S=1$	260	261	272	272	268	268	272	272
	$S=0$	232	228	208	208	212	212	208	208
$N=5$	$S=5/2$	100	100	98	98	102	98	98	98
	$S=3/2$	634	634	653	653	635	633	653	653
	$S=1/2$	1078	1078	1067	1067	1075	1081	1067	1067

III. RESULTS AND DISCUSSION

The photoemission spectrum is defined as

$$F_{\mathrm{PE}}(\omega,\mu\sigma) = \sum_k |\langle\phi^{N+1}_k|c^\dagger_{\mu\sigma}|\phi^N_0\rangle|^2\ \delta[\omega-(E^{N+1}_k - E^N_0)], \tag{3.1}$$

where ϕ^N_0 and ϕ^{N+1}_k are the N-hole ground state and the kth $(N+1)$-hole final state, with energies E^N_0 and E^{N+1}_k, respectively. The operator $c^\dagger_{\mu\sigma}$ creates a *hole* with spin σ on the orbital μ. The results can be added to get spin- and angle-resolved as well as integrated PES.

We have calculated the PES for an unsupported fcc Co(001) monolayer, one monolayer of Co on Cu(001) without and with the interface Co d–Cu s hybridization. In the case of Co/Cu(001) without the interface hybridization, all other parameters, including the crystal-field term contributed by the bulk Cu layers, are kept the same. We refer to these three structures as CoML, CoCuI (without the hybridization), and CoCuII hereafter. In the latter two cases, we concentrate on the PES contributed by the Co layer. This is done by applying the hole-creation operator to the orbitals on the Co atoms only, thus projecting out the PES from the Co layer. The sum rule of the spectral function is satisfied in all cases.

We first report the results for the unsupported Co(001) monolayer. The calculated spin-resolved and integrated PES of CoML corresponding to the $\bar{\Gamma}$ (normal emission) and $\bar{X}$ point are shown in Figs. 1 and 2. It is seen in Fig. 1 that there is a dominant peak near the Fermi level, followed by another rather strong peak at about 5.0 eV below the Fermi level with a long tail into the higher binding-energy region. The second peak is identified as a satellite peak, i.e., with peak energy higher than the bottom of the band predicted by single-particle theory, which is 4.2 eV. The characteristics of this spectrum are typical for strongly correlated itinerant magnetic systems.[9] Strong Coulomb interactions significantly reduce the probability of having two particles of opposite spin directions in the energy range close to the Fermi level. As a result, the peak near the Fermi level is highly polarized in the minority-spin orientation[17] with very small exchange splitting. At the same time, the spectral weight of majority-spin character is pushed by the interactions toward the higher binding-energy side, yielding the almost fully spin-polarized satellite peak with large exchange splitting. In Fig. 2, the PES with $\bar{X}$ symmetry

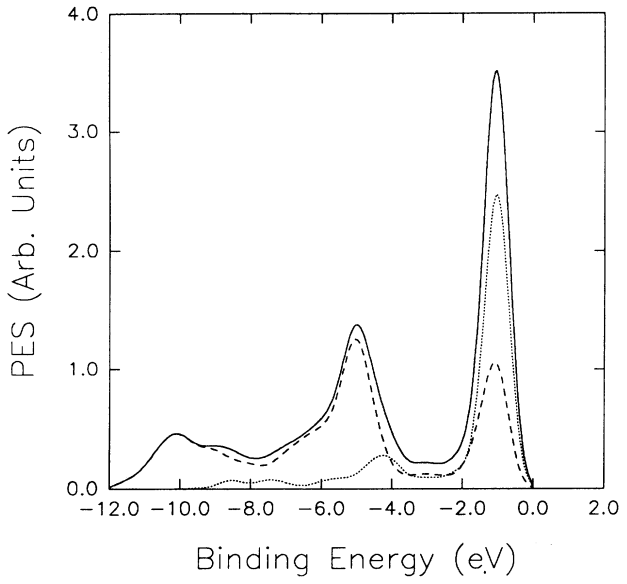

FIG. 1. The calculated spin-resolved normal-emission PES of the unsupported Co monolayer. The dashed and dotted curves represent results for majority- and minority-spin states. The solid curve is the spin-integrated result.

shows similar characteristics. However, there are some minor differences. First, the exchange splitting near the Fermi level is apparently larger, which is due to the fact that in the wave function with $\bar{X}$ symmetry there are larger probabilities of having particles distributed among different atoms, thus increasing the probability of having the particles with interaction energies close to the Fermi level. This leads to larger exchange splittings. Another observation is that the satellite peak at around 6.5 eV below the Fermi level (the single-particle band bottom projected onto the $\bar{X}$ point is 5.0 eV) is not well separated from the main-line part. Also, a stronger peak can be seen near the bottom of the spectrum.

We now turn to the results for the CoCuI structure, i.e., one-monolayer Co-on-Cu(001) substrate but *without* the interface *s-d* hybridization. The normal-emission PES has been reported (see Fig. 1 in Ref. 9). Figure 3 shows the calculated PES corresponding to the $\bar{X}$ point. In this structure, the crystal-field contribution from the Cu substrate is included, yielding a more bulk-like environment on one side of the Co monolayer. It is expected that the correlation effect should be weakened somewhat. Indeed, several indications of a weaker correlation effect are found in the spectra. First, the satellite structures move toward the lower binding-energy side, partly merging into the main line. Also, comparing the normal-emission results to Fig. 1, one sees an increased exchange splitting near the Fermi level, indicating a higher probability of having two particles on the same atom in that energy range and thus reduced correlation effects. The satellite peak previously located at 5.0 eV below the Fermi level has now largely merged into the the main-line part. On the other hand, a well-defined satellite peak is clear visible in the normal-emission spectrum at about 9.0 eV below the Fermi level. Similar conclusions can be drawn by comparing Fig. 3 to Fig. 2. However, there is an "anomaly" in Fig. 3; i.e., the exchange splitting near the Fermi level is smaller than that in Fig. 2. It should be pointed out that this is *not* an indication of increased correlation in the system.

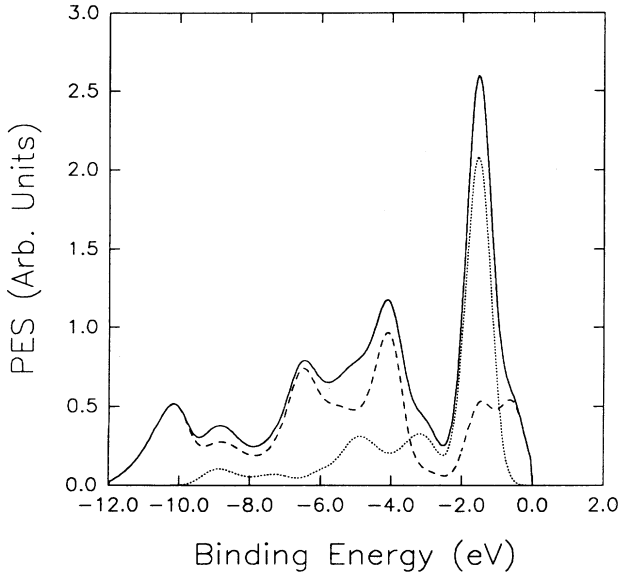

FIG. 2. Same as Fig. 1, but for PES of $\bar{X}$ symmetry.

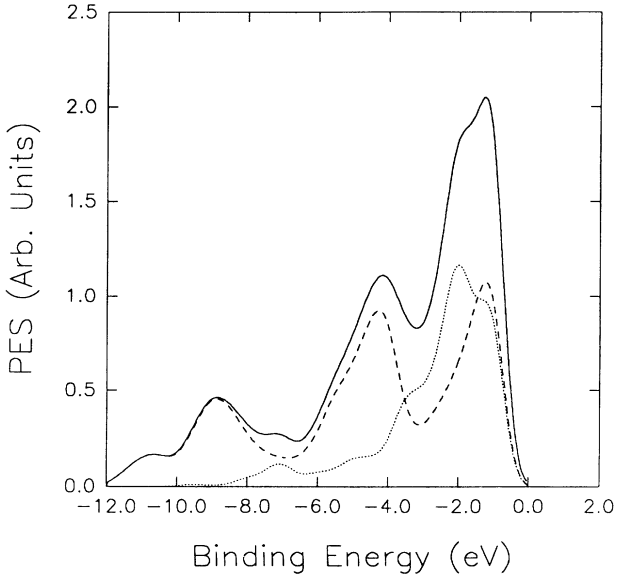

FIG. 3. The calculated spin-resolved PES with $\bar{X}$ symmetry of the one-monolayer Co on Cu(001) *without* the interface hybridization between the Co *d* and Cu *s* electrons. The dashed and dotted curves represent results for majority- and minority-spin states. The solid curve is the spin-integrated result.

A detailed analysis of the calculated electronic structure shows that this is actually due to some "unusual" shifts of the single-particle energy levels of $\bar{X}$ symmetry. It can be understood by making a Hubbard-model-like interpretation in which the single-particle levels are split by the exchange interaction J into single-particle majority-spin and minority-spin levels. This is, of course, only an approximate picture, since in the full many-body approach the configuration interaction mixes all single-particle levels; nevertheless, it is very useful in understanding the physics in the problem. In the normal-emission spectrum, the single-particle energy level shift alone is not enough to explain the increased exchange splitting near the Fermi level. It is thus an indication of decreased correlation effects. In Fig. 3 it leads to the above mentioned "anomaly." All the reported results are analyzed by making this Hubbard-model-like interpretation.

Finally, we turn to the interface *s-d* hybridization and study the photoemission spectra of the CoCuII structure. This structure corresponds to realistic one-monolayer Co on Cu(001). There are recent experimental *normal-emission* spectra available.[18] Our calculated results provide an explanation for the observed data.[9] Here we present in Fig. 4 the PES of $\bar{X}$ symmetry *projected from the Co atoms only.* Comparing with Fig. 3, one sees increased exchange splitting in the main-line part. Together with some restructuring of the single-particle energy levels, it leads to a double-peak structure near the Fermi level. More interestingly, there is a well-defined satellite peak located around 6.0 eV below the Fermi level. This peak has an almost neutral spin polarization, which is unusual for satellite structures in strongly correlated systems. High-resolution spin-polarized experiments should be able to test the calculated results.

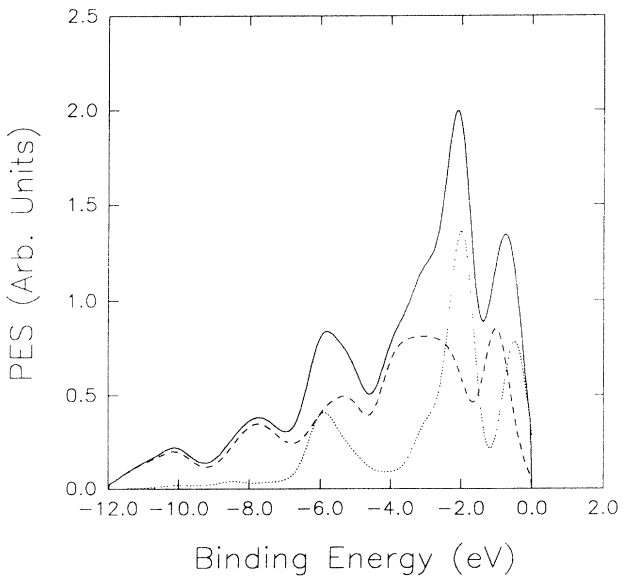

FIG. 4. The calculated spin-resolved PES with $\bar{X}$ symmetry of the one-monolayer Co on Cu(001) *with* the interface hybridization between the Co *d* and Cu *s* electrons. The dashed and dotted curves represent results for majority- and minority-spin states. The solid curve is the spin-integrated result.

IV. CONCLUSIONS

We have calculated spin- and angle-resolved photoemission spectra of three Co and Co/Cu systems to study the fundamental roles of the *d-d* correlation and the interface *s-d* hybridization of the strongly correlated two-dimensional itinerant magnetic system one-monolayer Co/Cu(001). Both single-particle band-structure results and many-body effects are considered on an equal footing in a periodic small-cluster approach. The exact diagonalization method is used to obtain all eigenvalues and eigenvectors. Photoemission spectra are calculated under the sudden (one-step) approximation. The results show that the correlation effect is quite strong in one-monolayer Co on Cu(001). It drives a significant amount of spectral weight beyond the energy range predicted by the sinlge-particle theory. The interface hybridization profoundly modifies the correlation effect. It enhances the exchange splitting near the Fermi level while reducing it at higher binding energies. In the normal-emission spectrum, the satellite structure is smoothed by the hybridization;[9] however, correlation-driven spectral weight transfer and spin polarization still should be observable in high-resolution spin-resolved photoemission experiments. On the other hand, the spectra of $\bar{X}$ symmetry show a well-defined satellite peak with almost neutral spin polarization. It should be easily detectable.

We conclude that both the correlation and the hybridization must be included in a many-body model and treated on an equal footing for interpreting the photoemission spectra of strongly correlated itinerant magnetic overlayer systems and for understanding the underlying physics. In general, the interface *s-d* hybridization tends to reduce the correlation effect, yielding larger exchange splitting in the spectrum near the Fermi level. It also causes shifts of satellite structures toward the lower binding-energy side. As a result of these spectral weight shifts, satellite structures may partly merge into the main-line part and, in some cases, may be smoothed out. The understanding of the detailed spectral function distribution requires a system-specific many-body calculation and a careful interpretation considering both single-particle effects and many-body effects.

ACKNOWLEDGMENTS

I would like to thank Jim Freericks for useful suggestions on improving the computer algorithm used in the calculation of the photoemission spectrum. This work was supported in part by a grant from Cray Research, and in part by the NSF under the EPSCoR program. Computation was carried out on the Cray YMP at the National Supercomputing Center for Energy and the Environment at UNLV.

[1] See, for example, L. M. Falicov, D. T. Pierce, S. D. Bader, R. Gronsky, K. B. Hathaway, H. J. Hopster, D. N. Lambeth, S. S. P. Parkin, G. Prinz, M. Salamon, I. K. Schuller, and R. H. Victora, J. Mater. Res. **5**, 1299 (1990), and references therein.

[2] C. Guillot *et al.*, Phys. Rev. Lett. **39**, 1632 (1977); D. E. Eastman *et al.*, *ibid.* **40**, 1514 (1978); F. J. Himpsel *et al.*, Phys. Rev. B **19**, 2919 (1979); L. A. Feldman and L. C. Davis, Phys. Rev. Lett. **43**, 151 (1979); W. Eberhardt and E. W. Plummer, Phys. Rev. B **21**, 3245 (1980); R. Clauberg *et al.*, Phys. Rev. Lett. **47**, 1314 (1981).

[3] D. R. Penn, Phys. Rev. Lett. **42**, 921(1979); A. Liebsch, *ibid.* **43**, 1431 (1979); N. Martensson and B. Johansson, *ibid.* **45**, 482 (1980); L. C. Davis and L. A. Feldkamp, Solid State Commun. **34**, 141 (1980); L. Kleinman and K. Mednick, Phys. Rev. B **24**, 6880 (1981); R. Clauberg, *ibid.* **28**, 2561 (1983); R. H. Victora and L. M. Victora, Phys. Rev. Lett. **55**, 1140 (1985).

[4] E. Dagotto, Rev. Mod. Phys. **66**, 763 (1994), and references therein.

[5] A. K. McMahan, R. M. Martin, and S. Satpathy, Phys. Rev. B **38**, 6650 (1988); M. S. Hybertsen, M. Schlüter, and N. E. Christensen, *ibid.* **39**, 9028 (1989); L. F. Mattheiss and D. R. Hamann, *ibid.* **40**, 2217, (1989); M. J. De Weert, D. A. Papaconstantopoulos, and W. E. Pickett, *ibid.* **39**, 4235 (1989); M. S. Hybertson, E. B. Stechel, M. Schlüter, D. R. Jennison, *ibid.* **41**, 11068 (1990).

[6] There are numerous papers on this subject. It is almost impossible to give an exhaustive list here. For a good review, see Ref. 4 and papers cited therein.

[7] Changfeng Chen, Int. J. Mod. Phys. B **5**, 1147 (1991), and references therein.

[8] Changfeng Chen, Phys. Rev. Lett. **64**, 2176 (1990); Phys. Rev. B **43** 6347 (1991); J. Phys. Condens. Matter **4**, 9855 (1992).

[9] Changfeng Chen, Phys. Rev. B **48**, 1318 (1993).

[10] For a review, see L. M. Falicov, in *Recent Progress in Many-Body Theories* edited by A. J. Kallio, E. Pajanne, and R. F. Bishop (Plenum, New York, 1988), Vol. 1, p. 275; J. Callaway, Physica B **149**, 17 (1988); Chen (Ref. 7).

[11] L. Smardz, U. Koebler, D. Kerkmann, F. Schumann, D. Pescia, and W. Zinn, Z. Phys. B **80**, 1 (1990).

[12] J. C. Slater and G. F. Koster, Phys. Rev. **94**, 1498 (1954).

[13] D. A. Papaconstantopoulos, *Handbook of the Band Structure of Elemental Solids* (Plenum, New York, 1986).

[14] C. Herring, in *Magnetism*, edited by G. T. Rado and H. Suhl (Academic, New York, 1966), Vol. 4.

[15] R. H. Victora, Ph.D. thesis, University of California, Berkeley, 1985 (unpublished). Although it is expected that the value of U may be enhanced at surfaces due to band narrowing, we find that it does not affect our results in any substantial way when the value of U increases a few eV from its bulk value. In principle, the d-d interaction may be reduced by the hybridization, thus yielding a featureless satelite tail in the photoemission spectrum. We did not explore this possibility in the present work. The value of U used in the calculation is consistent with the observed magnetization in the Co/Cu system *in the presence of hybridization.*

[16] M. Tinkham, *Group Theory and Quantum Mechanics* (McGraw-Hill, New York, 1964); A. W. Luehrmann, Adv. Phys. **17**, 1 (1968).

[17] Any use of words "majority" or "minority" in the context of the spin orientation refers to the electronic spin, not the spin of the hole. In particular, if the spins of all the holes in the ground state are the same, these holes are in a minority-spin state.

[18] W. Clemens, T. Kachel, O. Rader, E. Vescovo, S. Blügel, C. Carbone, and W. Eberhardt, Solid State Commun. **81**, 739 (1992).